Dual-responsive self-assembly of a bola-type supra-amphiphile constructed from a new pillar[6]arene-based recognition motif in water and its application in controlled release

Danyu Xia[a], Liqing Shangguan[a], Min Xue*[b] and Bingbing Shi*[a]

[a]*Department of Chemistry, Zhejiang University, Hangzhou 310027, P. R. China*
Fax: (+86) 571-87953189; Tel: +86-571-8795-3189; E-mail: bingbingshi@zju.edu.cn
[b]*School of Science, Zhejiang Sci-Tech University, Hangzhou 310018, P. R. China.*
Tel: +86-571-8684-3754; E-mail: minxue@zstu.edu.cn

Electronic supplementary information (14 pages)

1. Materials and methods

All reagents were commercially available and used as supplied without further purification. Compounds **WP6**,[S1] **a**[S2], **b**[S3] and **c**[S3] were prepared according to published procedures. NMR spectra were recorded with a Bruker Avance DMX 500 spectrophotometer or a Bruker Avance DMX 400 spectrophotometer. Low-resolution electrospray ionization mass spectra were recorded with a Bruker Esquire 3000 Plus spectrometer. High-resolution mass spectrometry experiments were performed with a Bruker 7-Tesla FT-ICR mass spectrometer equipped with an electrospray source (Billerica, MA, USA). The melting points were collected on a SHPSIC WRS-2 automatic melting point apparatus. UV-vis spectra were taken on a Perkin-Elmer Lambda 35 UV-vis spectrophotometer. Isothermal titration calorimetric (ITC) measurements were performed on a VP-ITC micro-calorimeter (Microcal, USA). The determination of the critical aggregation concentration (CAC) values was carried out on a DDS-307 instrument. Transmission electron microscopy investigations were carried out on a JEM-1200EX instrument. Atomic force microscopy (AFM) experiments were performed on a Multi-Mode Nanoscope-IIIa Scanning Probe Microscope (Veeco Company, USA) in the tapping mode. Dynamic light scattering was carried out on a Malvern Nanosizer S instrument at room temperature.

*2. Syntheses of **G** and **MG***

*2.1. Synthesis of **G***

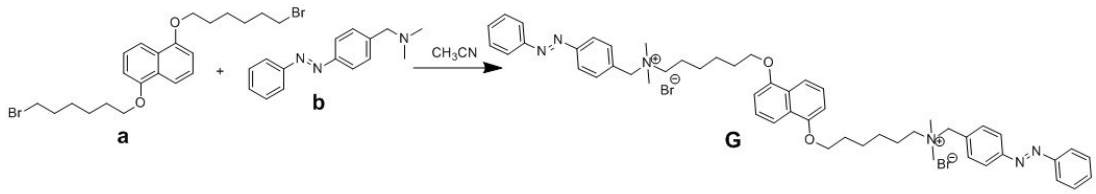

Scheme S1 Synthetic route to **G**

A mixture of **a** (1.52 g, 3.12 mmol), **b** (2.00 g, 9.36 mmol) was stirred in acetonitrile at 82 °C under N_2 atmosphere for 24 h. The precipitated product **G** was collected by filtration, washed with acetonitrile and dried under vacuum to obtain **G** as an orange solid (2.17 g, 72%). Mp: 142.2–144.9 ºC. The proton NMR spectrum of **G** is shown in Figure S1. ^{1}H NMR (400 MHz, DMSO-d_6, room temperature) δ (ppm): 7.99 (d, J = 8.4 Hz, 4H), 7.92 (dd, 4H), 7.78 (d, J = 8.4 Hz, 4H), 7.72 (d, J = 8.4 Hz, 2H),

7.68–7.59 (m, 6H), 7.38 (t, J = 4.2 Hz, 2H), 6.98 (d, J = 7.6 Hz, 2H), 4.66 (s, 4H), 4.14 (t, J = 6.0 Hz, 4H), 3.02 (s, 3H), 1.95–1.81 (m, 8H), 1.66–1.54 (m, 4H), 1.47–1.36 (m, 4H). The ^{13}C NMR spectrum of **G** is shown in Figure S2. ^{13}C NMR (100 MHz, DMSO-d_6, room temperature) δ (ppm):153.98, 152.59, 151.85, 134.20, 132.06, 131.10, 129.58, 125.47, 122.71, 122.69, 113.41, 105.65, 67.52, 65.57, 63.54, 49.25, 28.44, 25.34, 21.84. LRESIMS is shown in Figure S3: m/z 402.3 $[M - 2Br]^{2+}$ (100%). HRESIMS: m/z calcd for $[M - 2Br]^{2+}$ $C_{52}H_{64}N_6O_2$, 402.2545, found 402.2544, error 0 ppm.

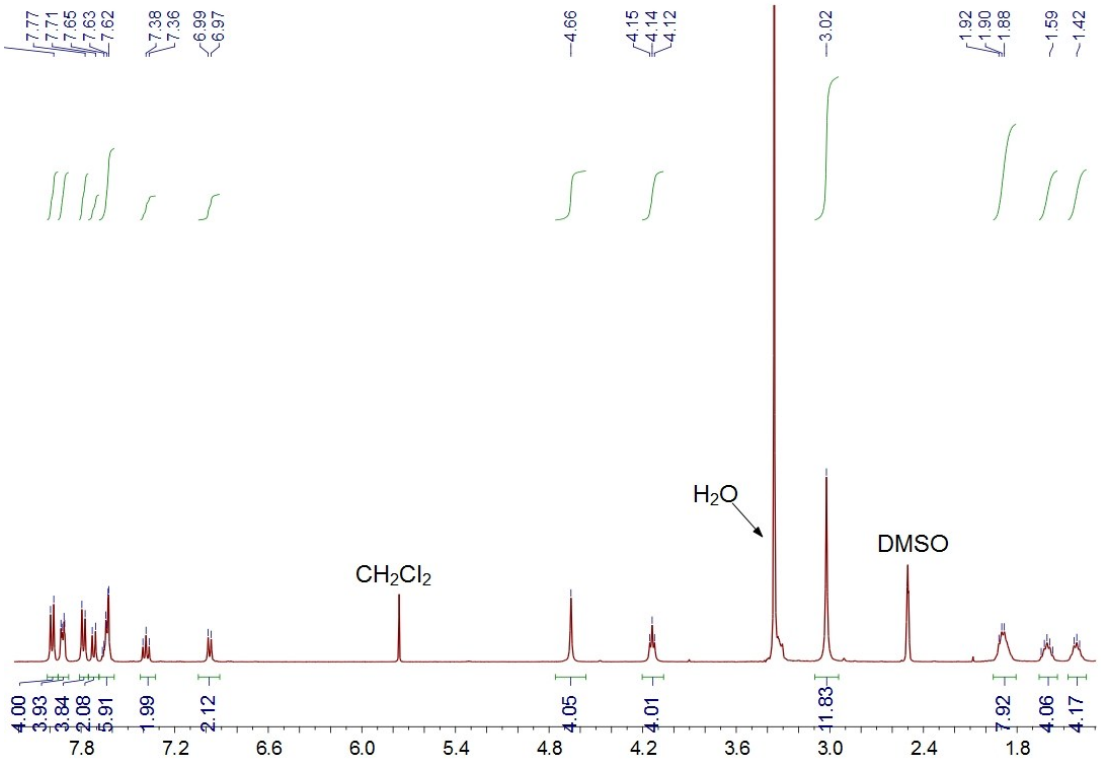

Figure S1 ^{1}H NMR spectrum (400 MHz, DMSO-d_6, 298 K) of **G**.

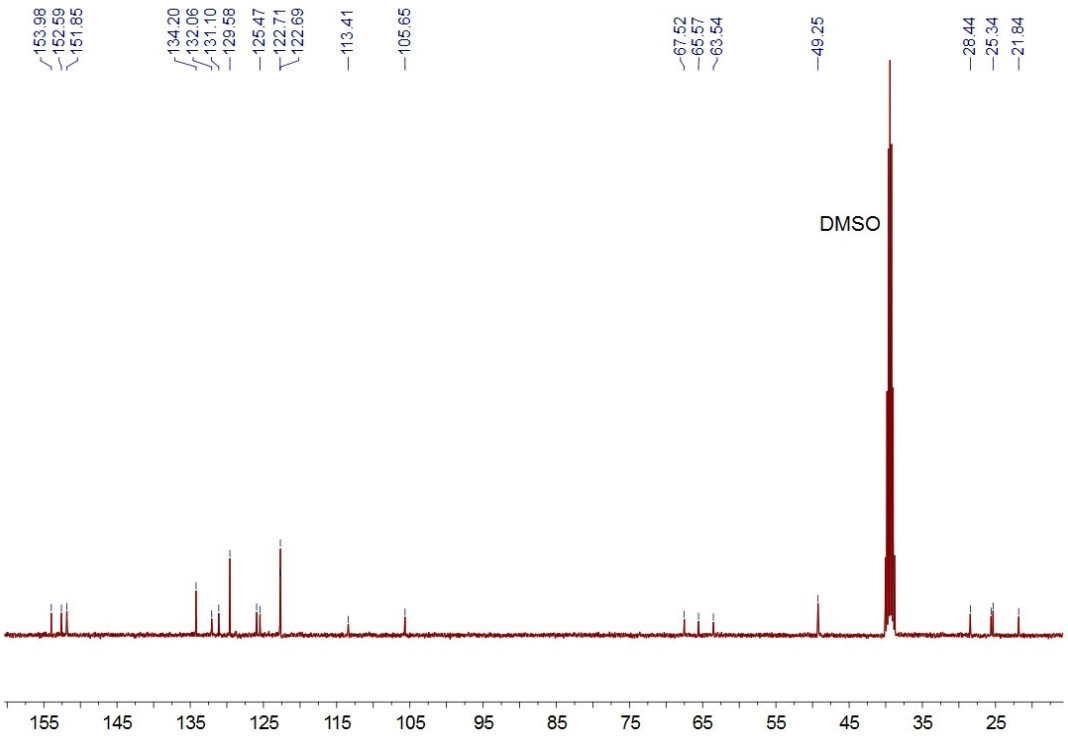

Figure S2 ^{13}C NMR spectrum (100 MHz, DMSO-d_6, 298 K) of **G**.

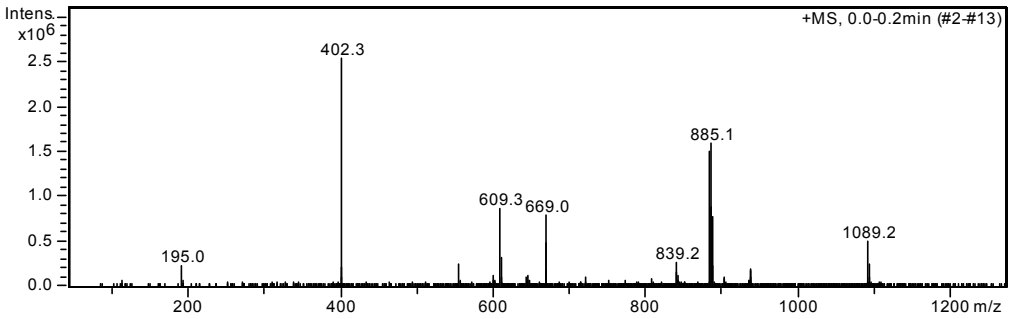

Figure S3 Electrospray ionization mass spectrum of **G**. Main peak: *m*/*z* 402.3 $[M - 2Br]^{2+}$ (100%).

*2.2. Synthesis of **MG***

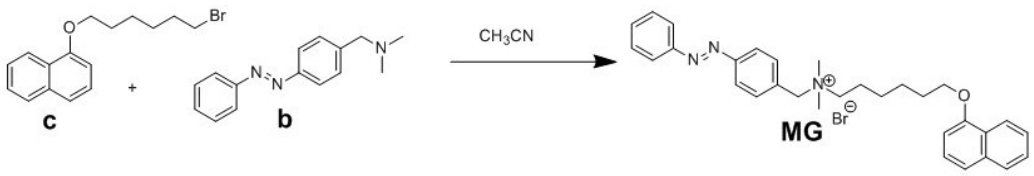

Scheme S2 Synthetic route to **MG**.

A mixture of **c** (1.25 g, 3.28 mmol), **b** (0.590 g, 3.28 mmol) was stirred in acetonitrile at 82 °C under N_2 atmosphere for 24 h. The precipitated product **MG** was collected by filtration, washed with acetonitrile and dried under vacuum to obtain **MG** as an orange solid (2.17 g, 72%). Mp: 175.3–177.1 ºC. The ^{1}H NMR spectrum of compound **MG** is shown in Figure S3. ^{1}H NMR (400 MHz, DMSO-d_6, 298 K) δ (ppm): 8.16 (dd, 1H), 7.99 (d, J = 8.4 Hz, 2H), 7.95–7.90 (m, 2H), 7.87 (dd, 1H), 7.79 (d, J = 8.4 Hz, 2H), 7.68–7.60 (m, 3 H), 7.55–7.48 (m, 2H), 7.48–7.39 (m, 2H), 6.97 (d, J = 6.8 Hz, 1H), 4.65 (s, 2H), 4.18 (t, J = 6.2 Hz, 2H), 3.02 (s, 6H), 1.99–1.79 (m, 4 H), 1.63–1.59 (m, 2 H), 1.52–1.35 (m, 2 H). The ^{13}C NMR spectrum of **MG** is shown in Figure S4. ^{13}C NMR (100 MHz, DMSO-d_6, 298 K) δ (ppm): 154.58, 153.17, 152.41, 134.75, 134.56, 134.01, 132.63, 130.15, 129.34, 128.04, 126.95, 126.81, 125.77, 125.46, 123.29, 123.24, 121.93, 120.66, 120.52, 120.32, 105.62, 68.03, 66.18, 64.17, 28.99, 26.16, 25.91, 22.40. LRESIMS is shown in Figure S5: m/z 466.3 [M – Br]$^+$ (100%). HRESIMS: m/z calcd for [M – Br]$^+$ $C_{31}H_{36}N_3O$, 466.2858, found 466.2853, error –1 ppm.

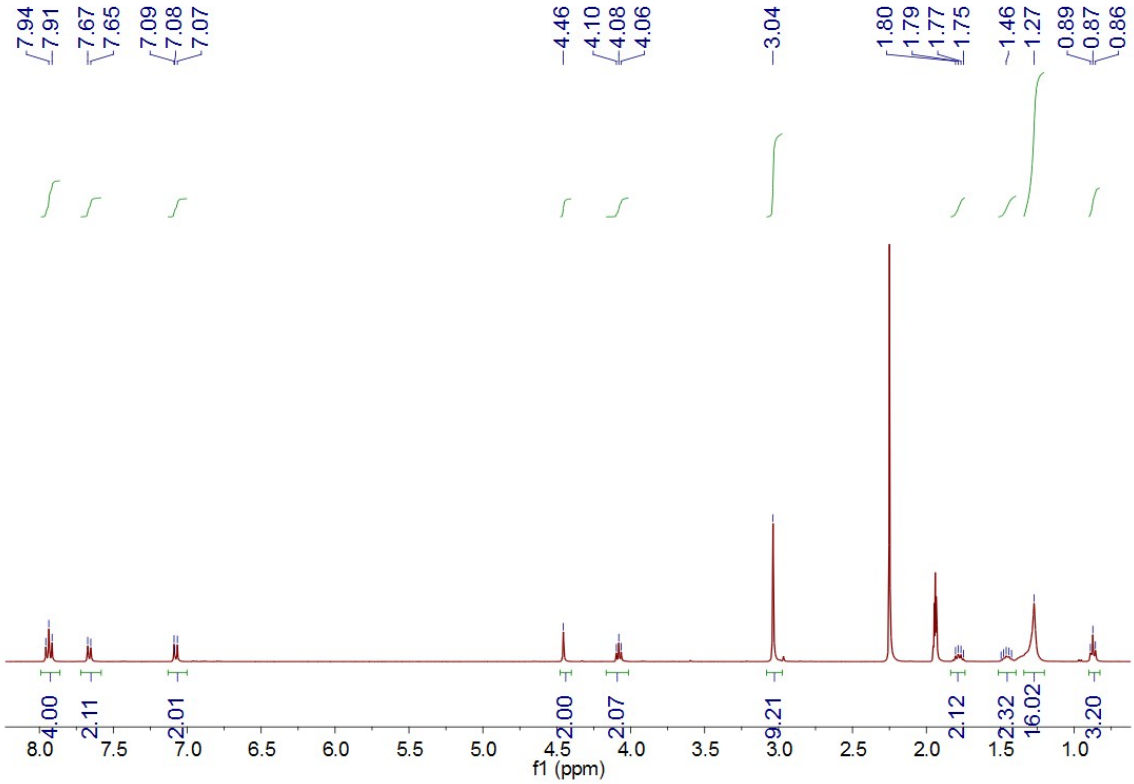

Figure S4 ^{1}H NMR spectrum (400 MHz, DMSO-d_6, 298 K) of **MG**.

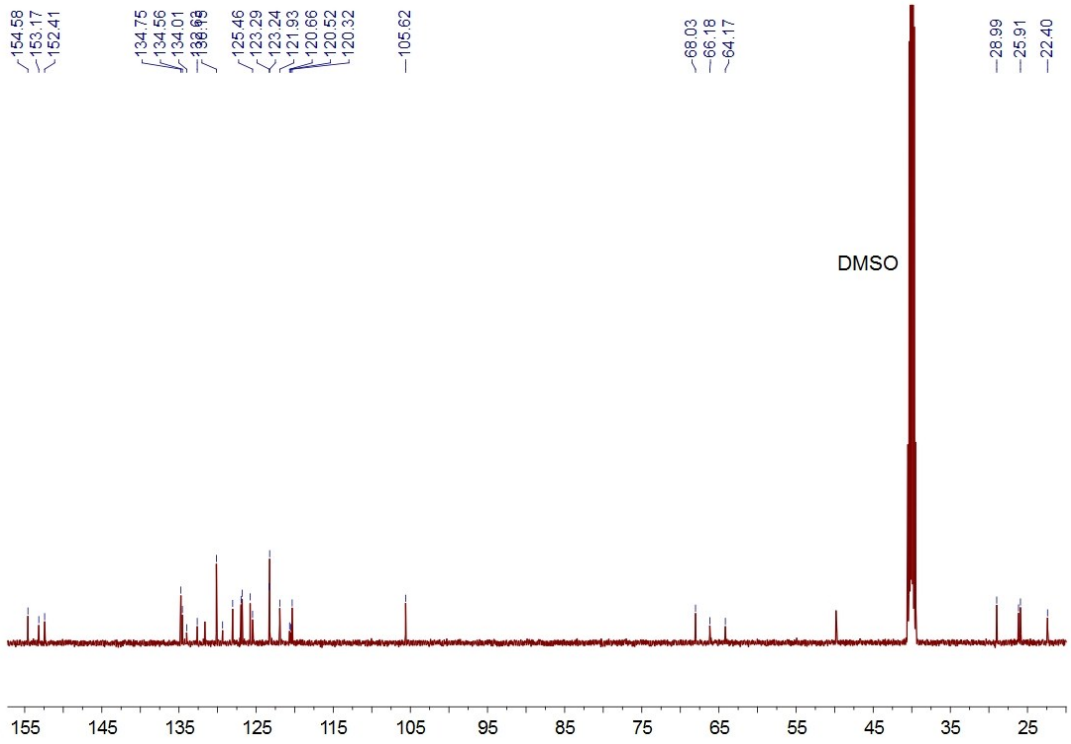

Figure S5 ^{13}C NMR spectrum (100 MHz, DMSO-d_6, 298 K) of **MG**.

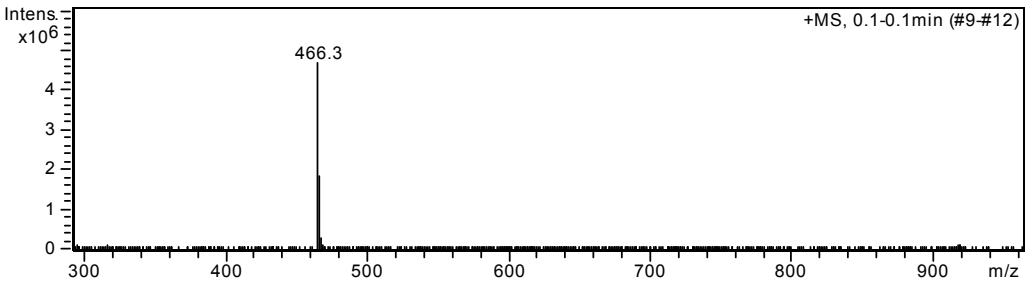

Figure S6 Electrospray ionization mass spectrum of **MG**. Main peak: *m*/*z* 466.3 $[M - Br]^+$ (100%).

*3. Partial 2 D NOESY spectra of an equimolar solution of **trans-MG** and **WP6***

2 D NOESY NMR experiment was employed to study the relative positions of the components in complex **WP6⊃*trans*-MG.** NOE correlation signals were observed between protons H_g of ***trans*-MG** and proton H_1 of **WP6** (Figure S7, A), between protons H_a, H_b, and H_c on the azobenzene unit of ***trans*-MG** and proton H_2 of **WP6** (Figure S7, B and C), and between protons H_g and H_h of ***trans*-MG** and proton H_3 of **WP6**.

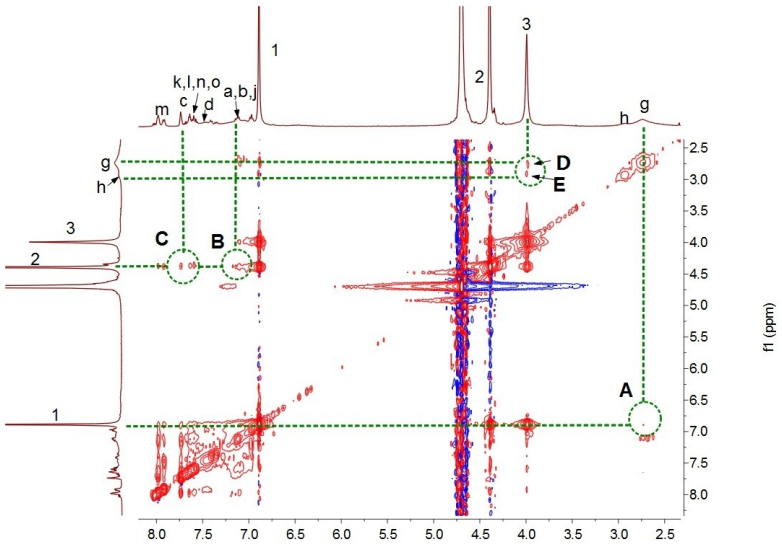

Figure S7 Partial 2D NOESY spectra (500 MHz, 3:1 D_2O/CD_3CN, room temperature) of an equimolar mixture ***trans*-MG** and **WP6** (2.50 mM).

*4. Isothermal titration calorimetry (ITC) experiment of **WP6** and **trans-G***

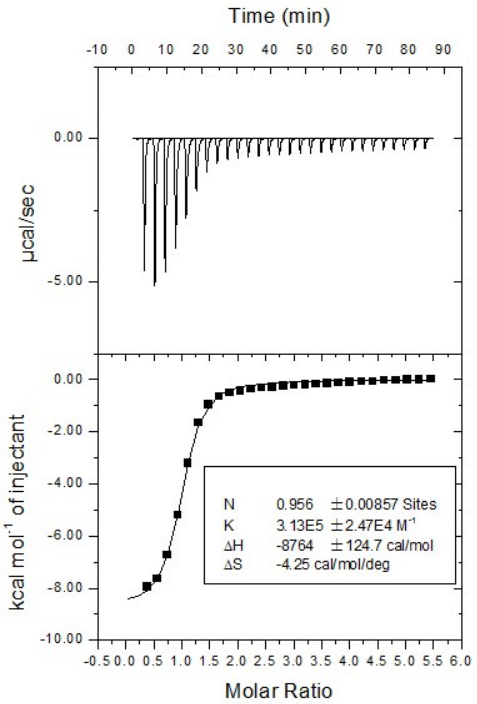

Figure S8 Microcalorimetric titration of **WP6** with ***trans*-MG** in water at 298.15 K. (Top) Raw ITC data for 29 sequential injections (10 µL per injection) of a **WP6** solution (2.00 mM) into a ***trans*-MG** solution (0.100 mM). (Bottom) Net reaction heat obtained from the integration of the calorimetric traces.

*5. pH-Responsive complexation of **WP6⊃trans-MG***

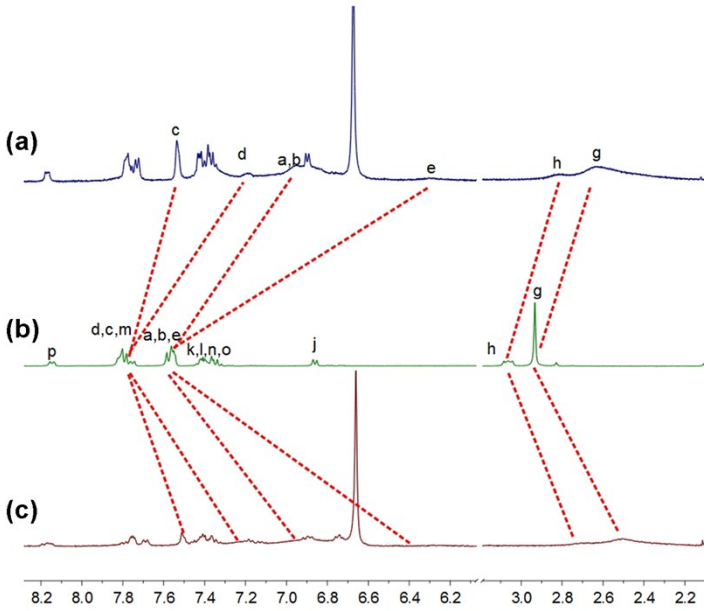

Figure S9 ^{1}H NMR spectra (500 MHz, 5:1 D_2O/CD_3CN, room temperature): (a) **WP6⊃*trans*-MG** (2.50 mM) when the solution pH was 7.0; (b) **WP6⊃*trans*-MG** (2.50 mM) when the solution pH decreased to 5.0; (c) **WP6⊃*trans*-MG** (2.50 mM) when the solution pH recovered to 7.0.

6. *Isothermal titration calorimetry (ITC) experiment of **WP6** and **trans-G***

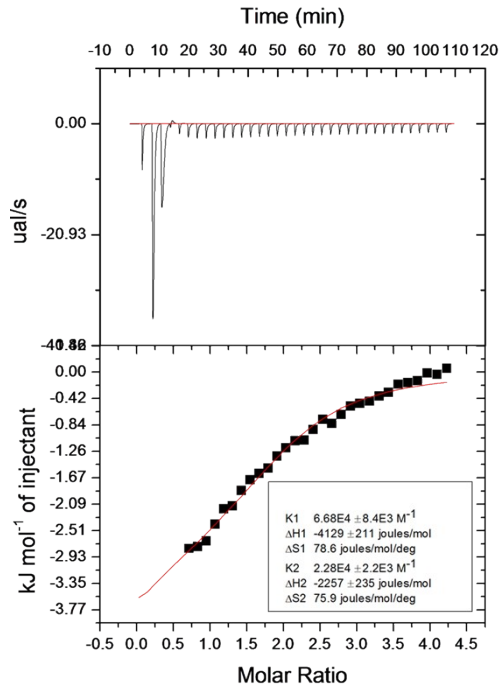

Figure S10 Microcalorimetric titration of **WP6** with ***trans*-G** in water at 298.15 K. (Top)

Raw ITC data for 29 sequential injections (10 μL per injection) of a **WP6** solution (2.00 mM) into a ***trans*-G** solution (0.100 mM). (Bottom) Net reaction heat obtained from the integration of the calorimetric traces.

7. UV-vis absorption spectroscopy experiments

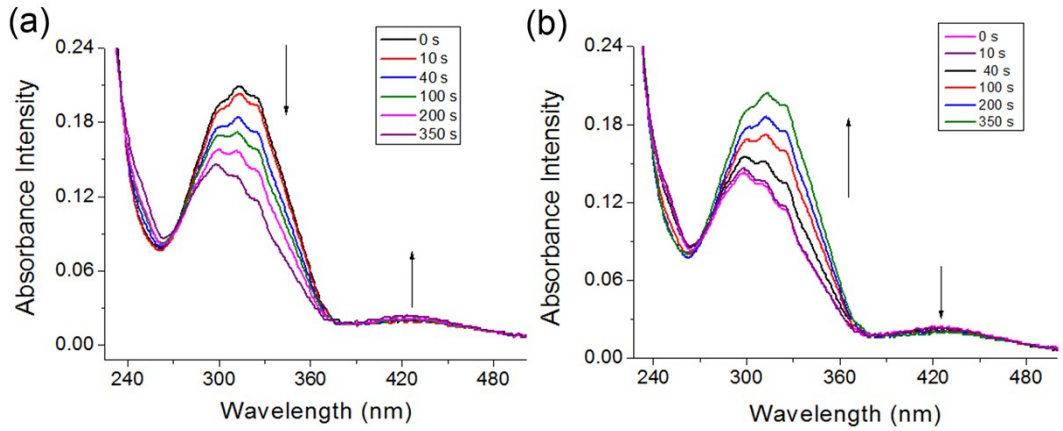

Figure S11 UV-vis absorption spectra of ***trans*-G** in water under UV irradiation at 365 nm from 0 to 350 s (a) and upon visible irradiation at 435 nm from 0 to 350 s (b). The concentration of ***trans*-G** was 2.50×10^{-5} M.

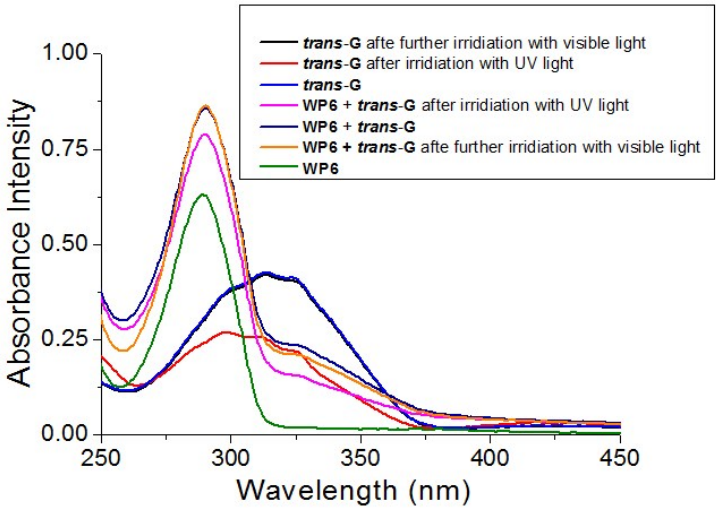

Figure S12 (a) UV-vis spectra of 2.50×10^{-5} M ***trans*-G** (initial and after irradiation with UV light at 365 nm for 10 min) and solution of 2.50×10^{-5} M ***trans*-G** and 5.00×10^{-5} M **WP6** (initial, after irradiation with UV light at 365 nm for 10 min, and then after irradiation with visible light at 435 nm for 10 min)

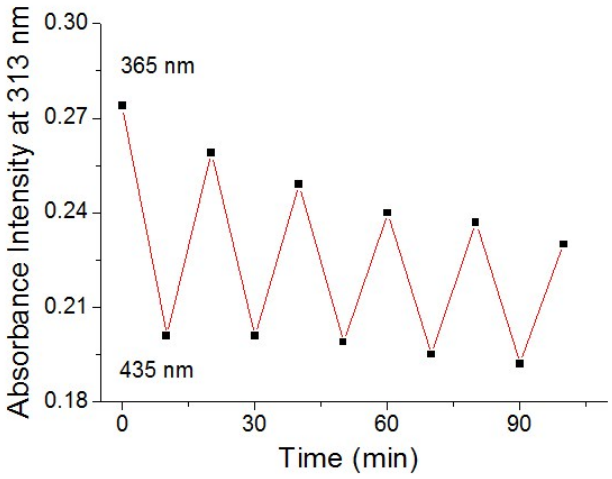

Figure S13 Changes of the absorbance at 313 nm of **(WP6)$_2$⊃G** upon alternating irradiation with UV and visible light for 10 min.

7. Critical aggregation concentration (CAC) determination of ***trans-G*** *and the equimolar mixture of* ***trans-G*** *and* ***WP6***

To measure the CAC values of ***trans-G*** and the equimolar mixture of ***trans*-G** and **WP6**, the conductivities of the solutions at different concentrations of ***trans*-G** and the equimolar mixture of ***trans*-G** and **WP6** were determined. By plotting the conductivity versus the concentration, we estimated the CAC values of ***trans*-G** and the mixture of ***trans*-G** and **WP6** (1:2 in ratio).

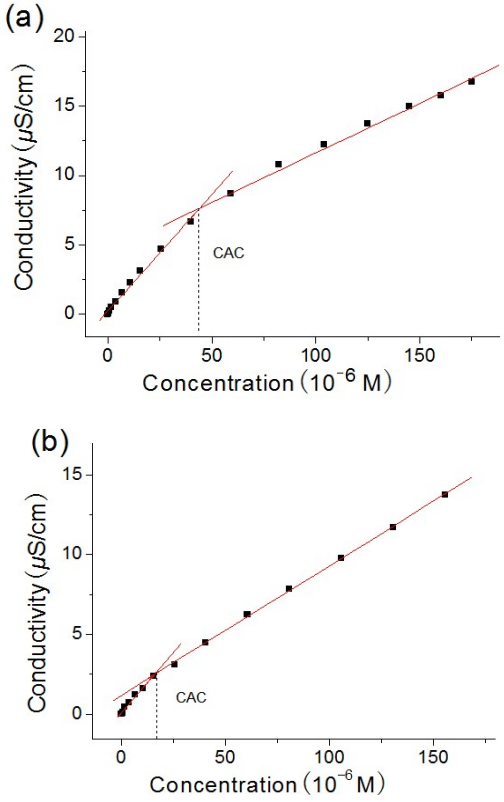

Figure S14 (a) Concentration-dependent conductivity of ***trans*-G**. The critical aggregation concentration (CAC) was determined to be 4.40 × 10^{-5} M; (b) Concentration-dependent conductivity of the mixture of ***trans*-G** and **WP6** (1:2 in ratio). The critical aggregation concentration (CAC) was determined to be 1.69 × 10^{-5} M of $(\mathbf{WP6})_2\supset\mathbf{G}$.

8. AFM results

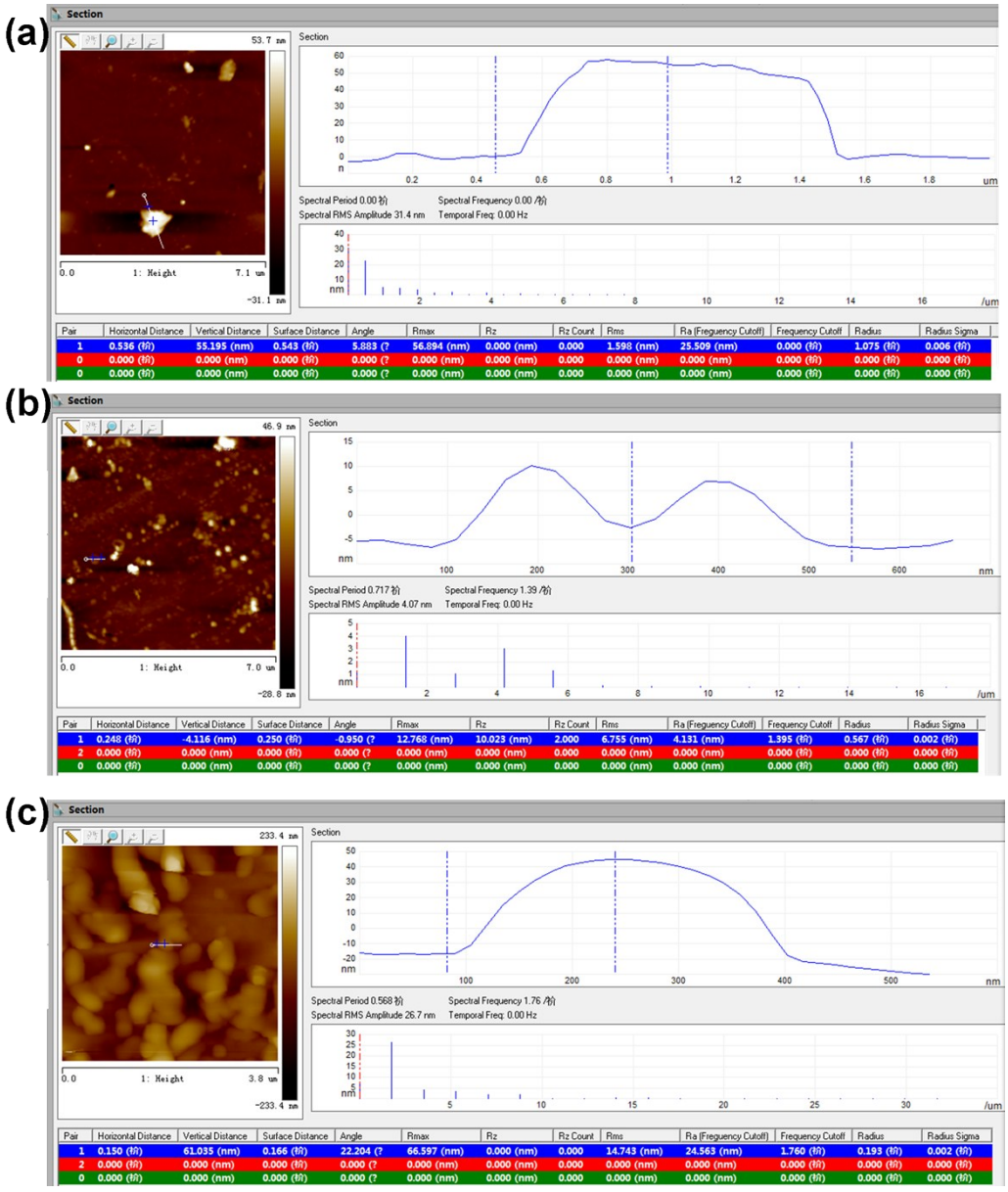

Figure S15 (a) AFM results of ***trans*-G** (2.50 × 10^{-5} M) aggregates in water; (b) AFM results of **WP6** (5.00 × 10^{-5} M) and ***trans*-G** (2.50 × 10^{-5} M for both) in water; (c) AFM results of the aggregates after irradiation with UV light at 365 nm of (b).

9. Dynamic light scattering (DLS) experitments

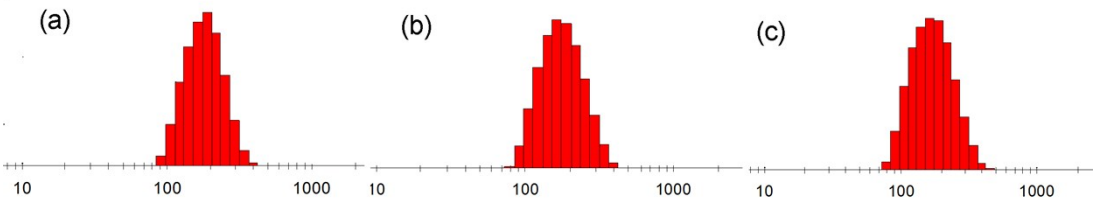

Figure S16 (a) DLS result of **WP6** with ***trans*-G** (2.50×10^{-4} M for both) in water; (b) DLS result of **WP6** with ***trans*-G** (2.50×10^{-4} M for both) in water after further irradiating with visible light at 435 nm; (c) DLS result of **WP6** with ***trans*-G** (2.50×10^{-4} M for both) in water after adding HCl solution and then adding NaOH solution.

10. DOX·HCl encapsulation and controllable DOX·HCl releaseexperiments

DOX·HCl loading experiment: DOX-loaded vesicles were prepared by adding a certain amount of DOX·HCl into a freshly prepared aqueous solution of **WP6** (5.00×10^{-5} M) and ***trans*-G** (2.5×10^{-5} M). The ultimate concentrations of DOX·HCl, **WP6**, and ***trans*-G** were 0.0500, 0.0500, and 0.02500 mM, respectively. And then the prepared DOX-loaded vesicles were purified by dialysis (molecular weight cutoff = 3500) in distilled water for several times until the water outside the dialysis tube exhibited negligible DOX·HCl fluorescence. As a result, DOX·HCl was successfully loaded into the vesicles constructed from **WP6⊃*trans*-G**-based bola-type supra-amphiphiles. The DOX·HCl encapsulation and loading efficiency were calculated by the following equations:[S3]

$$\text{Encapsulation Efficiency (\%)} = (m_{\text{DOX-loaded}}/m_{\text{DOX}})100$$

$m_{\text{DOX-loaded}}$ and m_{DOX} are mass of DOX·HCl encapsulated in vesicles and mass of DOX·HCl added, respectively. The mass of DOX·HCl was measured by a UV spectrophotometer at 490 nm and calculated as relative to a standard calibration curve in the concentrations from 2.00×10^{-6} to 4.00×10^{-5} M in water.

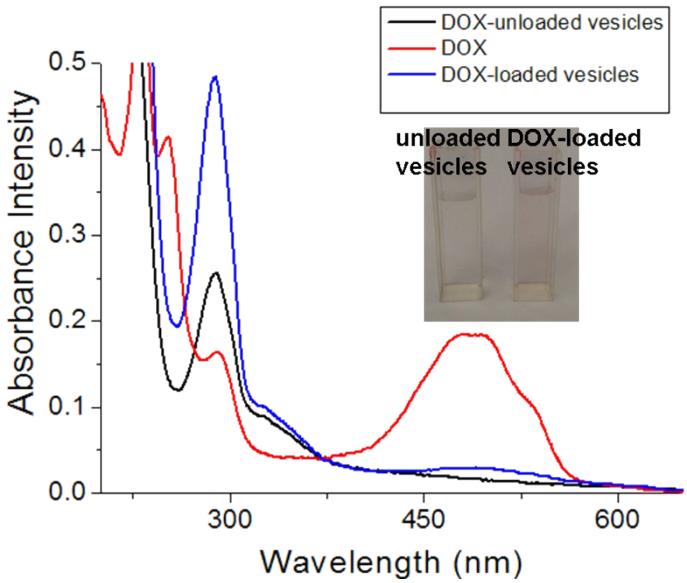

Figure S17 UV-vis absorption spectra of DOX-loaded vesicles, DOX·HCl, unloaded vesicles in water. Inset: color change of DOX-loaded vesicle (right) compared with unloaded one (left).

Controllable DOX·HCl release by pH changes: 0.05 M tris-HCl (pH = 7.4), 0.2 M sodium acetate (pH = 4.0), and 0.1 M citrate (pH = 6.5) buffer solutions were used as the release media. In a typical release experiment, 1.60 mL of DOX-loaded vesicles was added into 8.40 mL of appropriate release medium at 37 °C. At selected time intervals, 3 mL of the release media was taken out for measuring the released DOX·HCl concentrations by the UV-vis absorption technique and fluorescence emission spectrometer and then was returned to the original release media. The concentration of DOX·HCl was determined by measurement of absorbance at 490 nm using a standard absorbance verses concentration curve constructed for DOX·HCl in the corresponding release buffer. By presenting the vesicles to very low pH (the solution of HCl, pH = 2.0), a nearly 100% release of DOX·HCl from DOX-loaded vesicles could be obtained.

Controllable DOX·HCl release by photo irradiation: 0.05 M tris-HCl (pH = 7.4) buffer solutions were used as DOX·HCl release media. 1.60 mL of DOX-loaded vesicles was added into 8.40 mL of release medium at 37 °C. Upon irradiation with UV light at 365 nm, 3 mL of the release media at selected time intervals was taken out for measuring the released DOX·HCl concentrations by the UV-vis absorption technique and fluorescence emission spectrometerand then was returned to the original release media. The concentration of DOX·HCl was determined by measurement of absorbance at 490 nm using a standard absorbance verses concentration curve constructed for DOX·HCl in 0.05 M tris-HCl (pH = 7.4) buffer solutions.

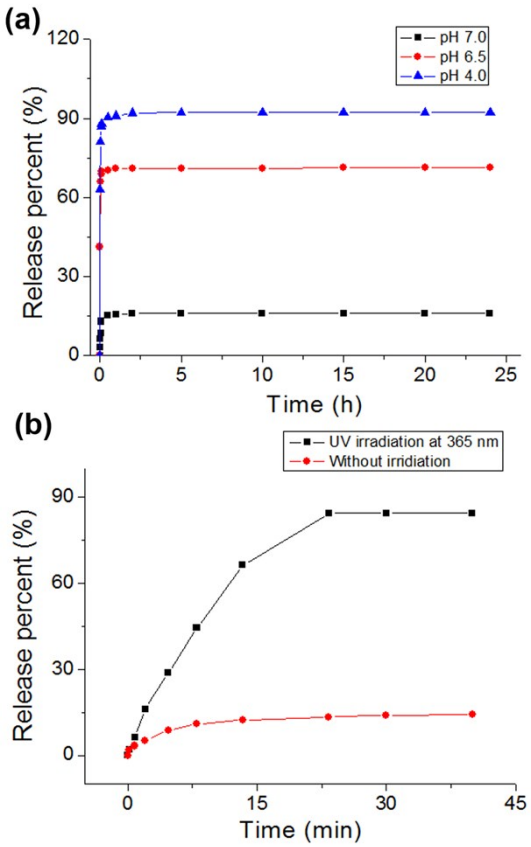

Figure S18 (a) Release percentage of the DOX-loaded vesicles in the release media of different pH values by fluorescence emission spectroscopy; (b) Release percentage of the DOX-loaded vesicles under the irradiation with UV light at 365 nm from 0 to 40 min by fluorescence emission spectroscopy.

References:

S1. D. Xia, G. Yu, J. Li and F. Huang, *Chem. Commun.*, 2014, **50**, 3606–3608.

S2. S. De and S. Ramakrishnan, *Chem. Asian J.*, 2011, **6**, 149–156.

S3. L. Peng, M. You, C. Wu, D. Han, I. Öçsoy, T. Chen, Z. Chen and W. Tan, *ACS Nano*, 2014, **8**, 2555–2561.

S4. S. Chambert, F. Thomasson and J.-L. Décout, *J. Org. Chem.*, 2002, **67**, 1898–1904.